MONTE CARLO EVALUATION OF NEOCLASSICAL TRANSPORT IN TORSATRONS WITH DIFFERENT HELICAL WINDING LAWS

C.D. Beidler, W.N.G. Hitchon[†], D.L. Grekov[‡], A.A. Shishkin[‡]

IPP 2/303 September 1989

MAX-PLANCK-INSTITUT FÜR PLASMAPHYSIK

8046 GARCHING BEI MÜNCHEN

MAX-PLANCK-INSTITUT FÜR PLASMAPHYSIK
Garching bei München

MONTE CARLO EVALUATION OF NEOCLASSICAL TRANSPORT IN TORSATRONS WITH DIFFERENT HELICAL WINDING LAWS

C.D. Beidler, W.N.G. Hitchon[†], D.L. Grekov[‡], A.A. Shishkin[‡]

IPP 2/303 September 1989

† *University of Wisconsin*
Department of Electrical and Computer Engineering
Madison, WI 53706, USA

‡ *Institute of Physics and Technology*
Academy of Sciences of the Ukrainian SSR
310108 Kharkov, USSR

Die nachstehende Arbeit wurde im Rahmen des Vertrages zwischen dem Max-Planck-Institut für Plasmaphysik und der Europäischen Atomgemeinschaft über die Zusammenarbeit auf dem Gebiet der Plasmaphysik durchgeführt.

MONTE CARLO EVALUATION OF NEOCLASSICAL TRANSPORT IN TORSATRONS WITH DIFFERENT HELICAL WINDING LAWS

Abstract

Neoclassical transport in realistic torsatron magnetic fields of reactor size is estimated by use of the Monte Carlo simulation technique. The configurations examined differ in the winding law which describes their helical conductors, a difference which has been analytically predicted to yield differing transport levels. This effect is confirmed not only in the $1/\nu$ regime, for which the analytic calculations were originally done, but at much lower collision frequencies as well. For the torsatrons examined, overall transport rates differ by a factor of 1.5 – 3. It is noted that the configuration with the more favorable transport characteristics bears some similarity to an Advanced Stellarator.

I. INTRODUCTION

The simplest model for the magnitude of the magnetic field in a toroidal stellarator or torsatron,

$$B/B_0 = 1 - \epsilon_t \cos\theta - \epsilon_\ell \cos(\ell\theta - m\phi),$$

is characterized by the fundamental helical harmonic with "wavenumbers" (ℓ, m). (In this equation, θ, ϕ are the poloidal and toroidal angles, respectively, ϵ_t is the inverse aspect ratio and ϵ_ℓ is the magnitude of the ℓ, m harmonic.) The generalization of this model field to include additional satellite harmonics,

$$B/B_0 = 1 - \epsilon_t \cos\theta + \sum_{n=0}^{\infty} \epsilon_{\ell\pm n} \cos\Big((\ell \pm n)\theta - m\phi\Big), \tag{1}$$

leads to the decreased (or increased) radial drift velocity of passing and trapped particles, resulting in the reduction (or growth) of the neoclassical transport coefficients. Whether the radial drift velocity decreases or increases depends on the signs of the ratios $\epsilon_{\ell\pm1}/\epsilon_\ell$, $\epsilon_{\ell\pm2}/\epsilon_\ell$, ...

This effect, the reduction of the radial drift velocity by a proper choice of additional satellite harmonics, was first shown in a model stellarator field which contained only the fundamental helical harmonic and its two nearest satellites, $(\ell\pm1, m)$ [1]. This same work presented numerical confirmation of the reduction of neoclassical transport rates for a drift-optimized stellarator field. Subsequent studies concentrated on analytical explanations of these favorable results [2-4] including their extension to an arbitrary number of satellite harmonics [3]. The important question of how a drift-optimized magnetic configuration could be achieved in an actual torsatron was also addressed [4-6]. A significant result to emerge from this work is that the satellite content of a torsatron's magnetic field can be controlled by a proper choice of the modulation coefficient, α, which appears in the winding law $(m/\ell)\phi = \theta - \alpha \sin\theta$ [4]. As α is varied in the range $-a/R \le \alpha \le a/R$ (here a is the minor radius of the helical windings and R is the major radius of the torus) the two satellites nearest to the fundamental harmonic change their signs from negative to positive. The geometrical factor D_0 which appears in the diffusion coefficient in the $1/\nu$ regime $D = D_0 v_T{}^4/(\omega_c{}^2\nu)$

$$D_0 = \epsilon_t{}^2 \epsilon_\ell{}^{3/2} \left[\gamma_1 - (\epsilon_\ell/\epsilon_t)\gamma_2 + (\epsilon_\ell/\epsilon_t)^2 \gamma_3\right]/r^2, \tag{2}$$

is especially sensitive to the sign of the nearest satellites (v_T is the thermal velocity, ω_c is the cyclotron frequency, ν is the 90 degree deflection frequency). The Fourier coefficients of B enter into D_0 through the quantities γ_1, γ_2 and γ_3 [6].

Simulations of neoclassical transport using various numerical approaches have all confirmed the favorable transport characteristics of drift-optimized configurations in the $1/\nu$ regime [7-9]. Moreover, it has been found that such configurations also provide a reduction in neoclassical transport rates in the range of still lower collision frequencies, i.e. in the $\nu^{1/2}$ and ν regimes [7,9]. These results have received further corroboration from an analytical solution of the bounce-averaged kinetic equation [9].

The investigations carried out in References [7-9] all dealt with the original model stellarator field [1] where only the two nearest satellite harmonics were present. It is therefore of some interest to perform similar Monte Carlo calculations allowing for the full harmonic content of actual torsatron configurations over the entire range of low collision frequencies. In particular, this will be done for two toratrons with $\ell = 2$, $m = 8$, $R/a \approx 3.6$, but with different modulation coefficients $\alpha = a/R \equiv \alpha^+$ and $\alpha = -a/R \equiv \alpha^-$.

The remainder of this paper is organized as follows: Section II introduces the magnetic field representation; Section III describes the Monte Carlo simulation and presents its results; Section IV provides a comparison with the existing analytic theory and a discussion of the results while the paper's conclusions will be given in Section V.

II. REPRESENTATION OF THE MAGNETIC FIELD

The vacuum magnetic fields of the two torsatron configurations (both with $R = 17$ m and $a = 4.7$ m) were calculated from the Biot-Savart Law. These configurations are similar to those studied in References [6,10] and possess, depending on the sign of α, different values of rotational transform. Note that these configurations have been chosen only as examples of torsatrons with opposite values of α; they are not optimized with respect to other magnetic field quantities (e.g. rotational transform, shear, radius of the last closed magnetic surface).

For several magnetic surfaces, the Fourier representation of B/B_0 is found in the Boozer coordinate set (r, ϕ, θ) [11] (where r is related to the toroidal flux, ψ, through the expression $\psi = B_0 r^2/2$) according to

$$B/B_0 = 1 + \sum_{M,N} A_{M,N}(r) \cos(N\theta + M\phi). \tag{3}$$

To complete the specification of the magnetic field, the Monte Carlo simulation requires analytic expressions for the radial dependence of each of the Fourier harmonics of B. For numerical efficiency, these expressions should be as simple as possible. We have therefore limited the expressions to the form $A_{MN} = c_2 + c_1\rho^c$, where $\rho = r/a_p$ is the minor radius normalized to the plasma radius and c, c_1, c_2 are constants to be determined for each harmonic. This simple form makes it impossible to accurately describe some harmonics at all radii; in such cases we have concentrated on the region near $\rho = .5$ since this is where the numerical simulation was carried out.

The model expressions used in the two cases were

$\alpha = a/R \equiv \alpha^+$	$\alpha = -a/R \equiv \alpha^-$
$-A_{0,1} = .104\rho$	$-A_{0,1} = .102\rho$
$A_{8,3} = .004\rho^2$	$A_{8,3} = .0228\rho^{2.1}$
$A_{8,2} = .0778\rho^2$	$A_{8,2} = .002 + .05\rho^2$
$A_{8,1} = -.0324 + .0914\rho^{0.4}$	$-A_{8,1} = .008 + .128\rho^{1.8}$
$A_{8,0} = .0211 - .018\rho^2$	$A_{8,0} = .0145 + .07\rho^2$
$-A_{8,-1} = .005\rho$	$-A_{8,-1} = .0008 + .0204\rho^{1.75}$
	$-A_{0,2} = -.0047 + .0112\rho^{0.5}$
	$A_{8,4} = .0131\rho^3$
	$A_{16,1} = .0002 + .0105\rho^{2.5}$
	$-A_{16,2} = .0001 + .0067\rho^{2.5}.$

The variation of the individual $A_{M,N}$ with ρ is given in Figures 1 ($\alpha = \alpha^+$) and 2 ($\alpha = \alpha^-$) by the solid lines. The dashed lines in these figures illustrate the analytic "fits" given above.

It is worth noting here that, unlike the model fields of earlier simulations, the fundamental harmonic is not necessarily the largest in magnitude. In fact, for the α^- configuration $|A_{8,1}|, |A_{8,0}| > |A_{8,2}|$ over the entire plasma cross section, and in the case of the α^+ configuration $A_{8,1}$ surpasses $A_{8,2}$ over the greater portion ($\rho \lesssim 0.8$) of the plasma column.

III. MONTE CARLO SIMULATION

Simulation parameters which are common to both magnetic field configurations are, major radius $R = 17$ m, minor radius of the helical windings $a = 4.7$ m, plasma minor radius $a_p = 1.6$ m, magnetic field on axis $B_0 = 4$ T, electrostatic potential profile $\Phi = \pm 11.3\ (1 - \rho^2)$ kV. The stationary background plasma was composed of equal densities of protons and electrons, each species at $T = 10$ keV. The collision frequency was altered by changing the densities. Test particles were monoenergetic protons with an energy corresponding to 12 keV; test particles were launched at $\rho = 0.5$. These parameters were chosen to facilitate comparison with the results of References [7-9] where neoclassical transport in reactor-sized stellarator/torsatrons was considered. As in these previous papers, the above parameters yield the drift scale length $|v_d/\Omega_E| = 0.08$, where $v_d = T/RB_0$ is the ∇B drift velocity and $\Omega_E = (-d\Phi/dr)/(rB_0)$ is the $\mathbf{E} \times \mathbf{B}$ precessional frequency. Note that for both configurations, a_p has been taken to be somewhat less than the radius of the last closed flux surface.

For the α^+ configuration the rotational transform on the launch surface is $\iota = 0.72$ and the geometrically averaged depth of the helical ripple on the launch surface (defined in the next section) is $\bar{\epsilon}_h = 0.0385$. For the α^- configuration $\iota = 0.435$ and $\bar{\epsilon}_h = 0.0466$.

The Monte Carlo numerical simulation used has been described previously [12]. However, because of the complicated magnetic field structures of the present configurations, it was impossible to run the Monte Carlo code in its "hybrid" formulation. Instead, it was run in a purely guiding center mode, or in a combined guiding center/free-streaming formulation. The former was used at high to intermediate collision frequencies, the latter at intermediate to very low collision frequencies. In the free-streaming region, a particle is constrained to follow the field line that it is currently on. This fast and simple description of a particle's trajectory is only used for completely passing particles; particles with low parallel velocity which can be reflected by the toroidal or helical ripples are always followed with guiding center equations.

Conventional analytic theory calculates a diffusion coefficient, D, for a given flux surface; i.e. D is a local quantity. Strictly speaking, the Monte Carlo simulation can only give an estimate of D because particles are free to drift off their original flux surface in the course of the simulation. To minimize this problem particles were restricted to the region $.25 < \rho < .75$. Particles reaching one of these boundaries were stopped. At very low collision frequencies in the α^+ configuration, a large fraction of the simulated particles (as high as 40%) reached one of these "cut-off" radii. This further complicates the estimate of a local diffusion coefficient; a statistical method for handling this situation is described in Reference [12].

Results are shown in Figures 3 ($\alpha = \alpha^+$) and 4 ($\alpha = \alpha^-$) with D plotted vs. ν_{eff}/Ω_E where $\nu_{eff} \equiv \nu/2\bar{\epsilon}_h$ is the "effective" collision frequency. Alternately, the second set of axes shows the diffusion coefficient normalized to the ion tokamak plateau value, D^*, and the mean free path normalized to half the connection length, L^* ($D^* = D/D_p$, where $D_p = 0.64\rho_L{}^2 v_T/(\pi R \iota\!\!\!-)$ with ρ_L the ion Larmor radius, and $L^* = \lambda/L_c$ with $L_c = \pi R/\iota\!\!\!-$). Monte Carlo numerical results are shown for both signs of electrostatic potential, $\Phi > 0$ (solid circles) and $\Phi < 0$ (open circles). To within the statistical uncertainty of the Monte Carlo method, no difference was noted in the results for the two signs of the electrostatic potential. As mentioned above, there were some difficulties in determining D at very low collision frequencies for the α^+ configuration. In these cases two data points are given which represent the estimates of the two different ways in which D was calculated.

IV. ANALYTIC THEORY AND DISCUSSION OF THE RESULTS

Also shown in the figures are analytic estimates of the diffusion coefficient. The dotted line shows the expected neoclassical transport rate [13] in the "equivalent" axisymmetric tokamak, i.e. a tokamak with the same aspect ratio and rotational transform. The solid line is an estimate of the transport level due to particles trapped in the helical ripples of the torsatron's magnetic field as given by a power-series solution of the bounce-averaged kinetic equation [9]. The dashed line is the sum of the dotted and solid lines.

The power-series solution cannot account for all the magnetic field harmonics present in the two current configurations, but it can handle the principal harmonics approximately in the following fashion. Using the method of Reference [3], one may approximate the magnetic field of both configurations by

$$B/B_0 = 1 + A_{0,1}\cos\theta + \epsilon_H \cos(\eta - \chi), \tag{4}$$

where

$$\epsilon_H = (\xi^2 + \gamma^2)^{1/2},$$

$$\xi = A_{8,1} + (A_{8,0} + A_{8,2})\cos\theta + (A_{8,-1} + A_{8,3})\cos 2\theta,$$

$$\gamma = (A_{8,0} - A_{8,2})\sin\theta + (A_{8,-1} - A_{8,3})\sin 2\theta,$$

$$\eta = \theta + 8\phi,$$

$$\cos\chi = \xi/\epsilon_H,$$

$$\sin\chi = \gamma/\epsilon_H.$$

The other, relatively small harmonics present in the α^- configuration have been ignored. Given these definitions, it is possible to define the geometrically-averaged depth of the helical ripple, introduced in the last section, as

$$\bar{\epsilon}_h = \frac{1}{2\pi}\int_0^{2\pi} \epsilon_H \, d\theta$$

For the α^+ case at $\rho = 0.5$, $\xi >> \gamma$ and ϵ_H is given to good approximation by $\epsilon_H = A_{8,1} + (A_{8,0} + A_{8,2}) \cos\theta$. The analytic theory [9] was developed for a helical-ripple profile of the form introduced in Reference [1], $\epsilon_H = \epsilon_h(1 - \sigma\cos\theta)$ which is precisely what is needed here given the identifications $\epsilon_h = A_{8,1}$ and $\sigma = -(A_{8,0} + A_{8,2})/A_{8,1}$. For the α^- configuration, the above approximations are not as good but may still be used to obtain a rough estimate of D. Incidentally, the above approximations yield $\bar{\epsilon}_h \approx A_{8,1}$, once again illustrating the subordination of the fundamental helical harmonic in these configurations.

As may be seen from the figures, agreement between the numerical and analytical results is reasonably good in both cases. It is, however, difficult to make a strong statement in the α^- case since the ripple transport is so much less than the axisymmetric transport except at very low collision frequency.

In earlier results, particle diffusion coefficients were determined for model torsatron fields with $\sigma = 0.4$ and $\sigma = -0.4$; a factor of three difference in D in the $1/\nu$ regime was predicted analytically for these configurations and confirmed by the numerical results [7,9]. Given the model field assumption it was possible to simulate both configurations with identical parameters, changing only the variation of B along a field line by switching the polarity of σ.

For the present torsatron configurations this is no longer true. The significant differences in the radial dependences of the individual Fourier harmonics of B insure that the two configurations will be quite dissimilar. This is manifested in the considerably different values of ι and $\bar{\epsilon}_h$ (the radius of the last closed flux surface is also different in the two cases although this difference had been avoided by setting $a_p = 1.6$ m in the numerical simulations). The large number of Fourier harmonics also limits the usefulness of the power-series analytical results which (1) assume only the fundamental helical harmonic and its two nearest satellites, and (2) further require that $\epsilon_{\ell+1} \approx \epsilon_{\ell-1}$. The first restriction is of some importance; previous asymptotic solutions of the kinetic equation in the $1/\nu$ regime have shown a deterioration of confinement when all satellite harmonics are accounted for [6,10]. Taking the present α^+ torsatron as an example, at $\rho = 0.5$ this configuration satisfies the above restrictions quite well and hence numerical and analytical estimates of D show very good agreement. At other radii, however, where the magnitudes of $A_{8,0}$ and $A_{8,2}$ differ considerably and where the remaining satellite harmonics become of significant amplitude, it is doubtful that the results would agree as well.

Nevertheless, the predictions of the power-series analytic theory are of considerable interest on two scores. First, they allow a comparison with previous analytic estimates of $1/\nu$ transport which also assumed only the fundamental harmonic and its two nearest satellites, and, more importantly, they provide the first estimate of the transport rates at very low collision frequencies where the $1/\nu$ scaling no longer holds. Given the identification of σ above, we obtain $\sigma = -0.98$ $(\alpha = \alpha^+)$ and $\sigma = 1.04$ $(\alpha = \alpha^-)$ for the present configurations. The power-series analytical diffusion curves obtained for these two values of σ and shown in Figures 3 and 4, predict an order of magnitude difference in ripple transport in the $1/\nu$ regime. This result agrees with those obtained earlier [6,10]. At yet lower collision frequencies the α^- torsatron continues to have the smaller ripple transport rate although the reduction is not as dramatic as in the $1/\nu$ regime. This result is also in agreement with those obtained previously for model magnetic fields [7,9].

The results obtained here are similar to those of other authors at higher collision frequencies as well. For the α^+ configuration, as for the conventional stellarator [11] and for a $\sigma = -0.4$ torsatron [8], the Monte Carlo simulation indicates a diffusion coefficient in the plateau regime that is larger than that of the equivalent tokamak. In contrast, the numerical results for the α^- torsatron lie slightly below those predicted for the equivalent tokamak. In this property, the α^- configuration is similar to an Advanced Stellarator [14].

The magnetic configurations considered here are torsatrons with moderate aspect ratio $(R/a = 3.6)$ and field period number $(m = 8)$. Currently, however, there is considerable interest in torsatrons with still smaller aspect ratio (2.5 – 3) and field period number (as few as 5) as a next step in stellarator efforts [15]. The ${\epsilon_t}^2$ scaling of D in the $1/\nu$ regime is an obstacle to the successful operation of such machines. Of particular interest in this regard are recent Monte Carlo simulations for Compact

Helical System (CHS) parameters ($R/a \approx 3$, $\alpha = 0.3$) [16]. A large ion loss cone was observed in these results, which was only closed by the presence of a significant electrostatic potential; electrons were found to obey the expected $1/\nu$ scaling. Since α is positive for CHS, it should be possible to improve on these results by using a smaller modulation coefficient in the winding law. Indeed, the results of Reference [16] showed increased particle confinement times when α was set equal to zero, even though this also caused a_p to shrink.

The last observation points out one of the present limitations of reducing neoclassical transport by modulating the winding law; namely that smaller plasma volumes tend to result. Because the slope of the helical windings is rather shallow on the outside of the torus, α^- torsatrons also have significantly more restricted experimental access. Finite plasma pressure has also been shown to degrade the confinement properties of the α^- configuration through an alteration of the harmonics present in the vacuum magnetic field [10]. A final drawback is that $\bar{\epsilon}_h$ tends to be larger in such devices as well; this point is of importance in future reactor considerations. As the present configurations have not undergone an optimization procedure, it is hoped that future research will be able to address these limitations.

V. CONCLUSIONS

(1) Neoclassical transport rates have been estimated for torsatrons with different winding laws using both analytical theory and the Monte Carlo numerical technique. Good agreement has been shown between the two approaches. For the current parameters, overall transport rates are reduced by a factor of 1.5 – 3 in favor of the $\alpha = -a/R$ configuration.

(2) Analytic estimates of the diffusion coefficient in the $1/\nu$ regime, based on consideration of the fundamental harmonic and its two nearest satellites, predict an order of magnitude difference for the two configurations. This is in agreement with previous analytical results. The degradation of confinement, predicted when further satellite harmonics are taken into account, was not observed numerically. This is

most likely due, however, to the simulation parameters; in the $\alpha = a/R$ case the additional satellites are not of concern at $\rho = 0.5$, while for $\alpha = -a/R$ the $1/\nu$ transport is masked by the axisymmetric contribution.

(3) At very low collision frequencies, where the $1/\nu$ scaling of the transport coefficients is no longer valid, the $\alpha = -a/R$ configuration continues to have the smaller diffusion rate, although the reduction is not as dramatic as in the $1/\nu$ regime.

(4) Besides having improved transport characteristics at low collision frequency, the $\alpha = -a/R$ torsatron exhibits a diffusion coefficient in the plateau regime which is less than that of the equivalent tokamak. In these two respects, it is similar to an Advanced Stellarator.

(5) Comparison of the results obtained here with those reported for CHS indicate that an optimized $\alpha < 0$ configuration could be of considerable interest as a candidate for a low-aspect-ratio torsatron experiment.

ACKNOWLEDGEMENTS

This work was carried out as part of a US-USSR exchange in fusion research and as part of an agreement on scientific and technical cooperation between the FRG and the USSR. The work of Dr. Hitchon was supported by DOE grant DE-FG02-85ER53201. We would also like to acknowledge the support and encouragement of Prof. O.S. Pavlichenko.

REFERENCES

[1] MYNICK, H.E., CHU, T.K., BOOZER, A.H., *Phys. Rev. Lett.* **48** (1982) 322.

[2] KOVRIZHNYKH, L.M., Transport Processes in Toroidal Magnetic Traps of Stellarator Type, Preprint FIAN No. 222, Moscow (1982) (in Russian). [See also: *Nucl. Fusion* **24** (1984) 851.]

[3] SHAING, K.C., HOKIN, S.A., *Phys. Fluids* **26** (1983) 2136.

[4] VOLKOV, E.D., SUPRUNENKO, V.A., SHISHKIN, A.A., in The Stellarator, Naukova Dumka, Kiev (1983) (in Russian).

[5] BYKOV, V.E., GEORGIEVSKIJ, A.V., PELETMINSKAYA, V.G., KHODYACHIKH, A.V., SHISHKIN, A.A., *Pis'ma Zh. Tekh. Fiz.* **10** (1984) 749 (in Russian). [English Translation: *Sov. Tech. Phys. Lett.* **10** (1984) 314.]

[6] BYKOV, V.E., GEORGIEVSKIJ, A.V., PELETMINSKAYA, V.G., KHODYACHIKH, A.V., SHISHKIN, A.A., *Nucl. Fusion* **24** (1984) 1195.

[7] HITCHON, W.N.G., MYNICK, H.E., *J. Plasma Phys.* **37** (1987) 383.

[8] SHAING, K.C., HIRSHMAN, S.P., BEASLEY, C.O., JR., CRUME, E.C., JR., VAN RIJ, W.I., in Plasma Physics and Controlled Nuclear Fusion Research 1986 (Proc. 11th Int. Conf. Kyoto, Japan, 1986), Vol. 2, IAEA, Vienna (1987) 391.

[9] BEIDLER, C.D., HITCHON, W.N.G., VAN RIJ, W.I., HIRSHMAN, S.P., SHOHET, J.L., *Phys. Rev. Lett.* **58** (1987) 1745.

[10] BYKOV, V.E., GREKOV, D.L., SHISHKIN, A.A., GARCIA, L., HARRIS, J.H., ROME, J.A., *Nucl. Fusion* **28** (1988) 871.

[11] BOOZER, A.H., KUO-PETRAVIC, G., *Phys. Fluids* **24** (1981) 851.

[12] BEIDLER, C.D., HITCHON, W.N.G., SHOHET, J.L., *J. Comput. Phys.* **72** (1987) 220.

[13] ROSENBLUTH, M.N., HAZELTINE, R.D., HINTON, F.L., *Phys. Fluids* **15** (1972) 116.

[14] BROSSMAN, U., DOMMASCHK, W., HERRNEGGER, F., GRIEGER, G., KISSLINGER, J., LOTZ, W., NÜHRENBERG, J., RAU, F., RENNER, H., RINGLER, H., SAPPER, J., SCHLÜTER, A., WOBIG, H., in Plasma Physics and Controlled Nuclear Fusion Research 1982 (Proc. 9th Int. Conf. Baltimore MD, USA, 1982), Vol. 3, IAEA, Vienna (1983) 141.

[15] CARRERAS, B.A., DOMINGUEZ, N., GARCIA, L., LYNCH, V.E., LYON, J.F., PAINTER, S.L., SHEFFIELD, J., TOLLIVER, J.S., CARY, J.R., HANSON, J.D. presented at the 12th Int. Conf. Plasma Physics and Controlled Nuclear Fusion Research, Nice, France, 1988 (to be published).

[16] CHEN, T.S., Monte Carlo Analysis of Neoclassical Transport for a Compact Helical System, Preprint IPPJ-850, Nagoya, Japan (1987).

FIGURE CAPTIONS

FIGURE 1 The radial dependences of the magnetic field harmonics of the $\alpha = a/R$ torsatron are shown (solid lines) according to the Fourier representation given in equation (3). The dashed lines indicate the numerical fits given in the text which were used as input for the Monte Carlo simulation. The amplitudes of all harmonics are normalized to B_0, the plasma radius is $a_p = 1.6$ m.

FIGURE 2 As in Figure 1 for the $\alpha = -a/R$ torsatron.

FIGURE 3 The diffusion coefficient, D, is plotted against normalized collision frequency, ν_{eff}/Ω_E, for the $\alpha = a/R$ torsatron described in the text. The second set of axes presents the results as diffusion coefficient normalized to the ion plateau value, D^*, against mean free path normalized to half the connection length, L^*. The dotted line indicates the expected transport level in the equivalent tokamak [13] while the solid line is an estimate of the ripple transport obtained from a power-series solution of the bounce-averaged kinetic equation [9]. The dashed line is the sum of the solid and dotted lines. Monte Carlo numerical results are shown for ($\bullet$) $\Phi > 0$, and ($\circ$) $\Phi < 0$.

FIGURE 4 As in Figure 3 for the $\alpha = -a/R$ torsatron described in the text.

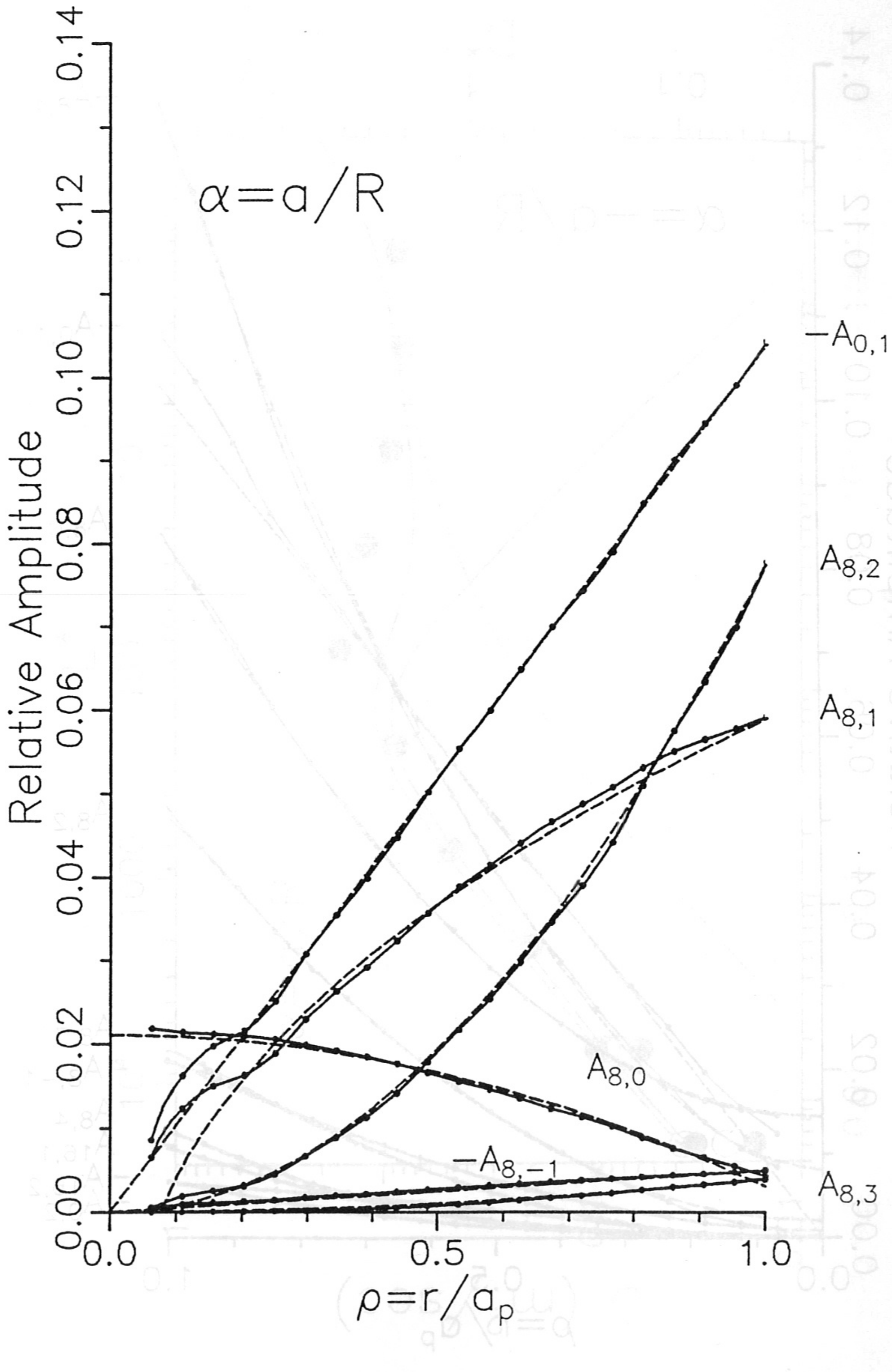

$\alpha = a/R$
$-A_{0,1}$
$A_{8,2}$
$A_{8,1}$
$A_{8,0}$
$-A_{8,-1}$
$A_{8,3}$
Relative Amplitude
0.00
0.02
0.04
0.06
0.08
0.10
0.12
0.14
0.0
0.5
1.0
$\rho = r/a_p$

FIGURE 1

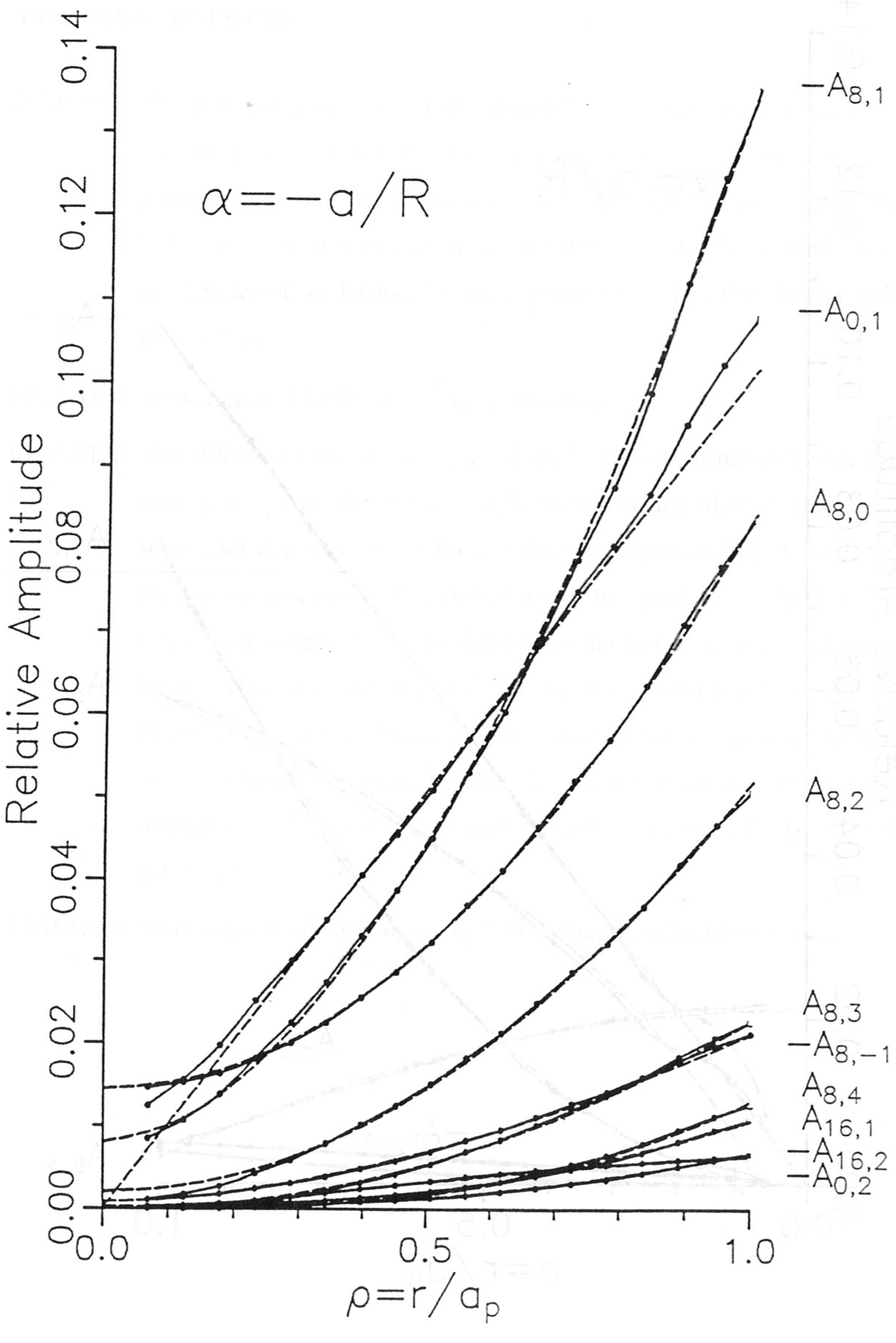
α=−a/R
Relative Amplitude
0.00
0.02
0.04
0.06
0.08
0.10
0.12
0.14
0.0
0.5
1.0
ρ=r/a_p
−A8,1
−A0,1
A8,0
A8,2
A8,3
−A8,−1
A8,4
A16,1
−A16,2
−A0,2

FIGURE 2

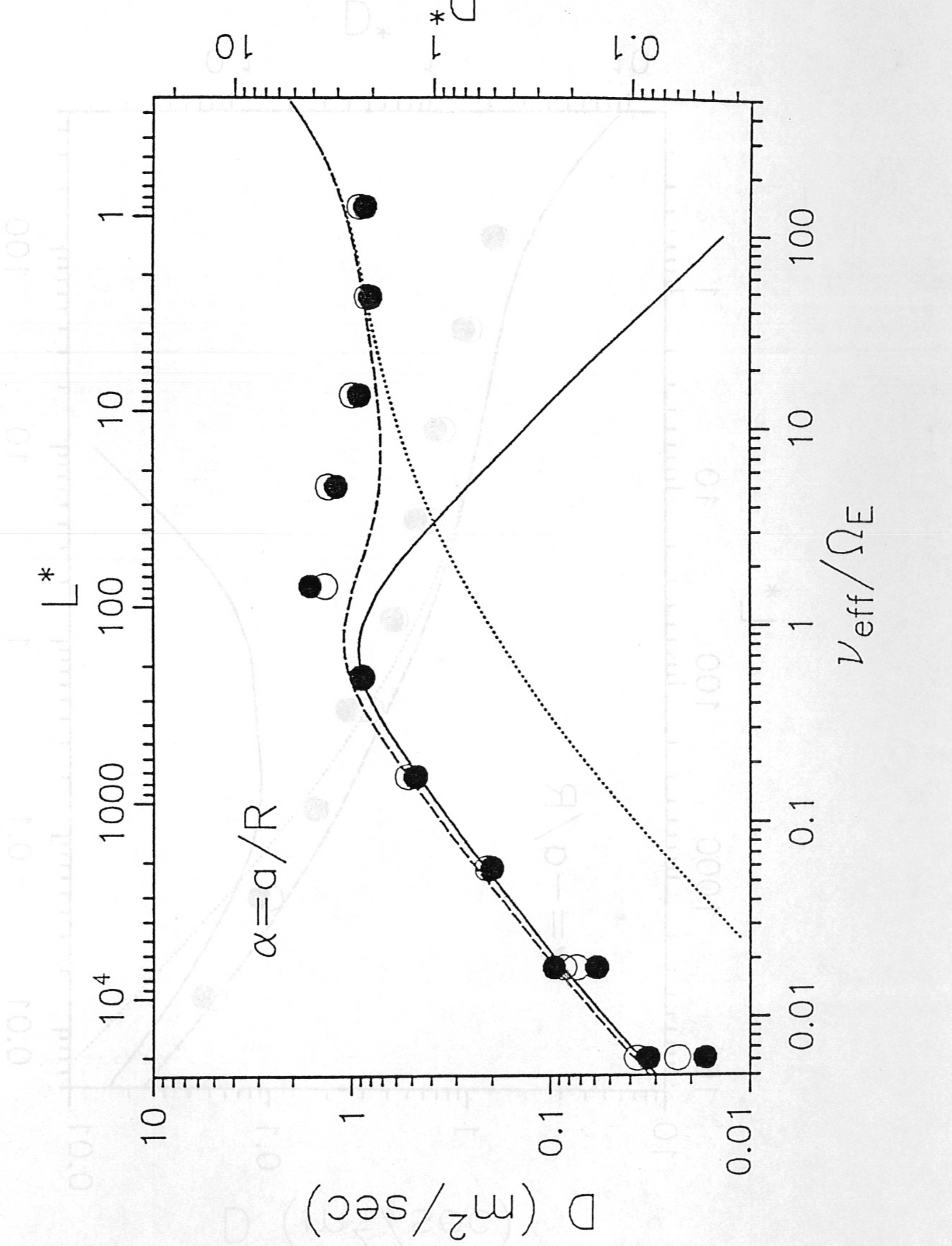
L*
D*
α=a/R
D (m²/sec)
ν_eff/Ω_E
10
1
0.1
0.01
10⁴
1000
100
10
1
10
1
0.1
0.01
0.1
1
10
100

FIGURE 3

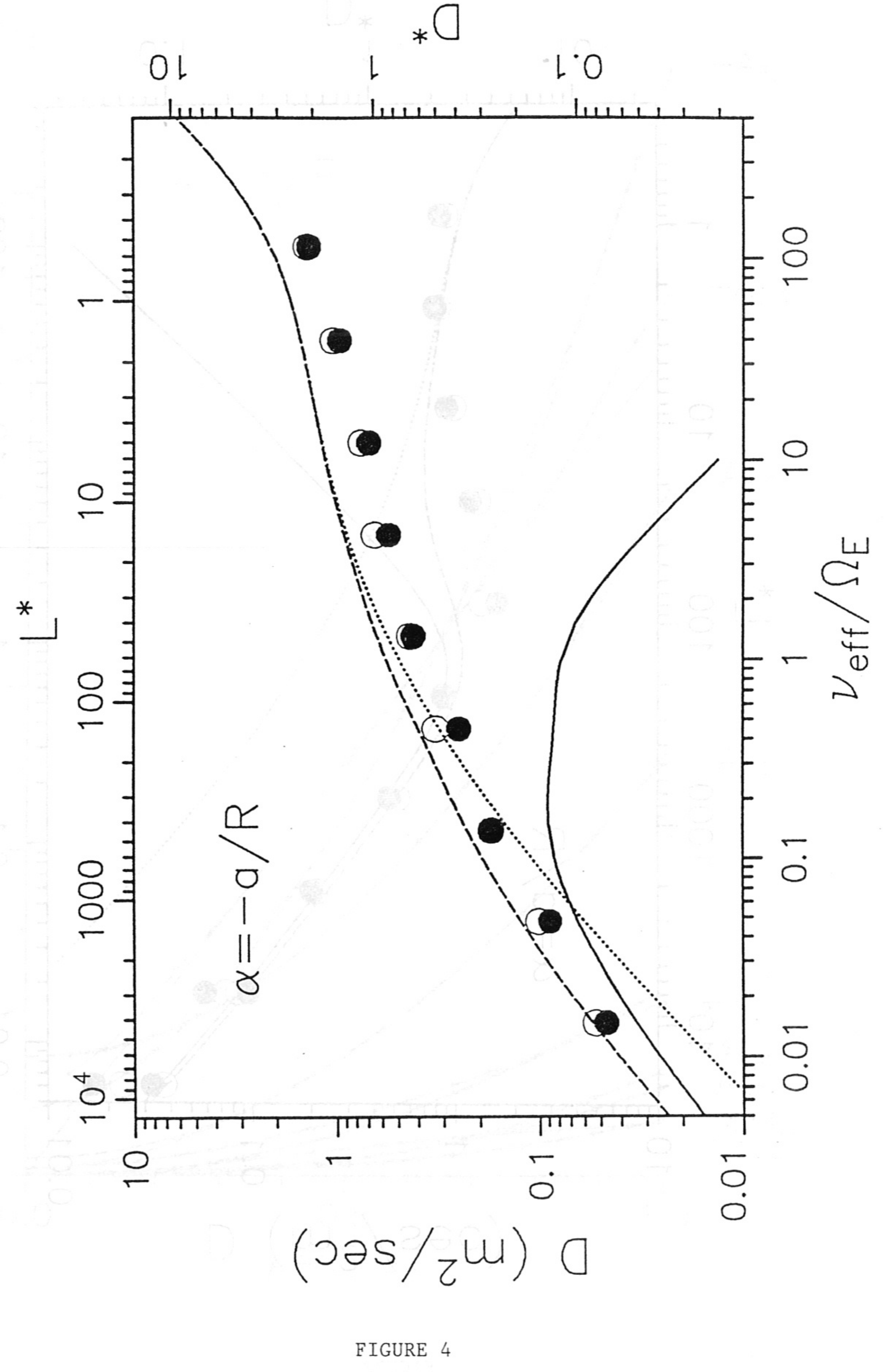

FIGURE 4